THE JOURNAL OF PHYSICAL CHEMISTRY A

Article

pubs.acs.org/JPCA

Intrinsic Autocorrelation Time of Picoseconds for Thermal Noise in Water

Zhi Zhu,[†,‡] Nan Sheng,[†,‡] Rongzheng Wan,[†] and Haiping Fang*[,†]

[†]Division of Interfacial Water and Key Laboratory of Interfacial Physics and Technology, Shanghai Institute of Applied Physics, Chinese Academy of Sciences, P.O. Box 800-204, Shanghai 201800, China

[‡]University of Chinese Academy of Sciences, Beijing 100080, China

Supporting Information

ABSTRACT: Whether thermal noise is colored or white is of fundamental importance. In conventional theory, thermal noise is usually treated as white noise so that there are no directional transportations in the asymmetrical systems without external inputs, since only the colored fluctuations with appropriate autocorrelation time length can lead to directional transportations in the asymmetrical systems. Here, on the basis of molecular dynamics simulations, we show that the autocorrelation time length of thermal noise in water is ∼10 ps at room temperature, which indicates that thermal noise is not white in the molecular scale while thermal noise can be reasonably assumed as white in macro- and meso-scale systems. The autocorrelation time length of thermal noise is intrinsic, since the value is almost unchanged for different temperature coupling methods. Interestingly, the autocorrelation time of thermal noise is correlated with the lifetime of hydrogen bonds, suggesting that the finite autocorrelation time length of thermal noise mainly comes from the finite lifetime of the interactions between neighboring water molecules.

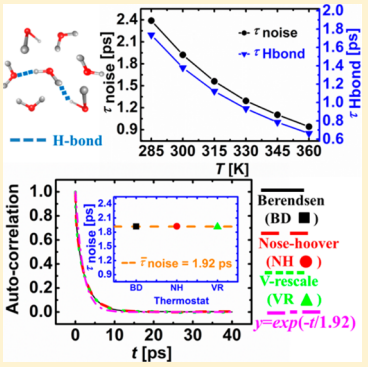

INTRODUCTION

Nanoscale systems usually display behaviors different from those of bulk systems.[1−7] In 1997, Kelly et al. designed a molecule containing triptycene with helicenes and observed spontaneous unidirectional rotations of the triptycene over a short time period without any input of external colored fluctuations.[8−10] It is clear that if all the fluctuations in their systems, mainly thermal noise,[11] are white, there will not be unidirectional rotations of the triptycene over a finite time period. In recent years, unidirectional transportations of water induced by electrostatic fields have also been observed in molecular dynamics (MD) simulations without any input of external colored fluctuations,[12−14] and there are great debates on the existence of these unidirectional transportations.[15−19] On the basis of the traditional theory, there is not biased transportation in the system with spatial asymmetry without any external input, since thermal noise is regarded as white.[20] On the characters of thermal noise, in 1994, Magnasco argued that the autocorrelation time length of thermal noise should be smaller than ∼100 ps.[21] We have shown that the finite autocorrelation time length of thermal noise was the key to the directional transportation in nanoscale,[22] and the autocorrelation time length of thermal noise of bulk water in the MD simulations with Nose−Hoover thermostat was ∼10 ps. MD simulation is widely used in studying nanoscale systems,[23−32] there are many computational methods to maintain a constant temperature in MD simulation, which are referred as the temperature coupling methods or the thermostats. Since the colored noise with certain autocorrelation time length coupling with appropriate asymmetrical potential may induce unidirectional transportation,[20,22] it is of great importance to make clear whether the finite autocorrelation time length of thermal noise is intrinsic or results from the computational methods, as well as the mechanism underlying the observed autocorrelation time length.

In this paper, we showed that the finite autocorrelation time length of thermal noise is intrinsic of ∼10 ps at room temperature, based on MD simulations on water. The autocorrelation time lengths of thermal noises are almost unchanged for the typical temperature coupling methods, including Berendsen,[33] Nose−Hoover,[34,35] and V-rescale thermostats.[36] We found that the autocorrelation time length of thermal noise depended on the reference temperature. Interestingly, the hydrogen bonds had similar autocorrelation behavior as thermal noise in MD simulations, which suggests that the finite autocorrelation time length of thermal noise mainly comes from the finite lifetime of the interactions between neighboring water molecules.

METHOD

The MD simulations were carried out with the initial box size $L_X = L_Y = L_Z = 3.0$ nm by Gromacs 4.5.5,[37] with 895 TIP3P[38] rigid water molecules, as TIP3P water model is widely used in

Special Issue: International Conference on Theoretical and High Performance Computational Chemistry Symposium

Received: January 28, 2014
Revised: June 18, 2014
Published: June 18, 2014

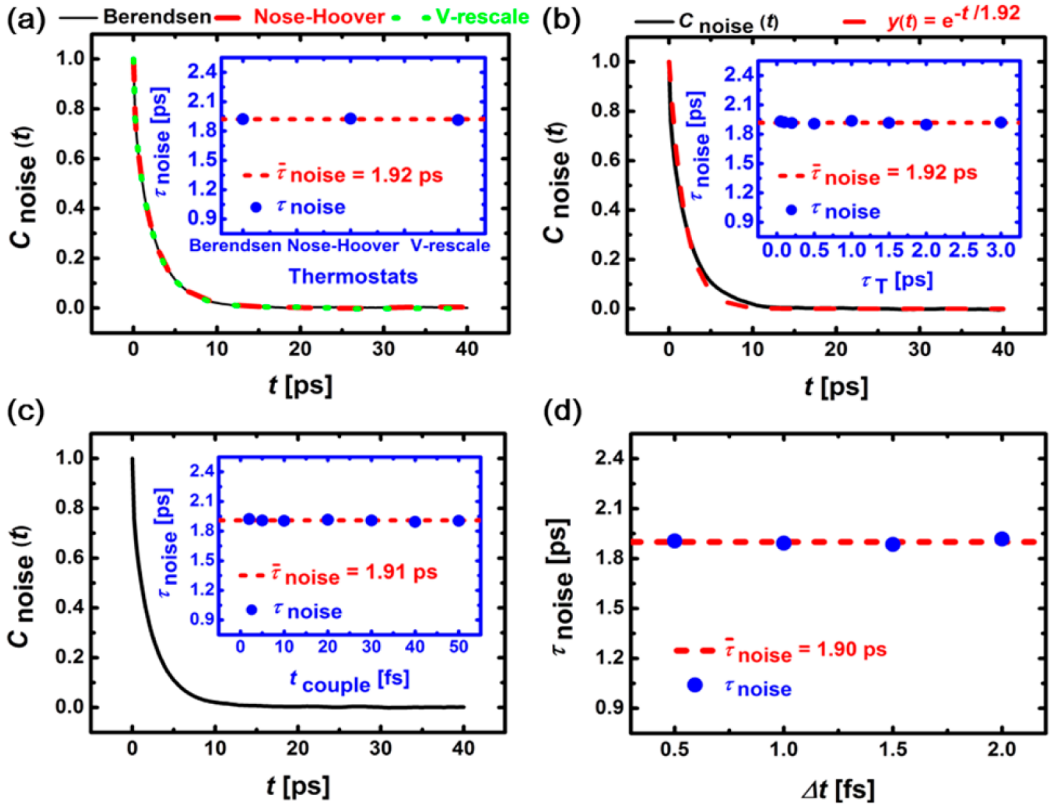

Figure 1. Autocorrelation functions of thermal noise $C_{noise}(t)$ and their characteristic time τ_{noise} at 300 K for different computational methods. (a) Autocorrelation functions of thermal noise $C_{noise}(t)$ with Berendsen (black solid line), Nose−Hoover (red dash line), and V-rescale thermostats (green dot line). Inset is the characteristic time τ_{noise} (blue solid circle) of $C_{noise}(t)$ for different thermostats with τ_T = 0.1 ps and t_{couple} = 2 fs at 300 K. The red dash line shows the average value $\overline{\tau}_{noise}$ = 1.92 ps. (b) $C_{noise}(t)$ for Nose−Hoover thermostat (black solid line) with the time constant for coupling τ_T = 0.1 ps, together with the exponential fit $y(t) = \exp(-t/\tau_{noise})$ (red dash line), where the τ_{noise} = 1.92 ± 0.02 ps. Inset is the characteristic time τ_{noise} of $C_{noise}(t)$ for different τ_T (the blue solid circle), and the red dash line shows the average value $\overline{\tau}_{noise}$ = 1.92 ps. (c) $C_{noise}(t)$ (black solid line) with the period for coupling t_{couple} = 2 fs. Inset is τ_{noise} (blue solid circle) for different t_{couple}, and the red dash line shows the average value $\overline{\tau}_{noise}$ = 1.91 ps. (d) τ_{noise} (blue solid circle) for different simulation time step Δt with τ_T = 0.2 ps and t_{couple} = 6 fs. The red dash line shows the average value $\overline{\tau}_{noise}$ = 1.90 ps.

studying the liquidity and transport property of water.[12,39−42] Periodic boundary conditions were applied in all directions. The Parrinello−Rahman pressure coupling[43,44] has been used to maintain the system pressure at 1 bar. The Berendsen, Nose−Hoover, and V-rescale thermostats have been used to maintain the reference temperature. The particle mesh Ewald (PME) integration[45] was used to treat the long-range electrostatic interactions. The simulation time for each system was 20 ns, with a time step of 2 fs. The trajectory has been collected every 0.2 ps, and the data of last 10 ns have been extracted to analyze the characteristics of thermal noise.

We used the fluctuating force ζ that exerts on the water O atom from surrounding water molecules in MD simulation to characterize thermal noise. The autocorrelation function[22] of ζ is

$$C_{noise}(t) = \frac{\langle \zeta(0)\zeta(t)\rangle}{\langle \zeta(0)\zeta(0)\rangle} \tag{1}$$

Here, $\zeta(0)$ and $\zeta(t)$ are the forces that are exerted on the oxygen atom at time 0 and t. An exponential function $y(t) = e^{-t/\tau_{noise}}$ was used to fit the autocorrelation function $C_{noise}(t)$, where τ_{noise} was defined as the characteristic time of thermal noise.

For the Nose−Hoover thermostat, there are two very important coupling parameters: the time constant for coupling τ_T and the period for coupling t_{couple}. Berendsen and V-rescale thermostats have the same two coupling parameters. (The details of Berendsen and V-rescale thermostats are discussed in Supporting Information as section I.) When the Nose−Hoover temperature coupling method is applied, the equation of motion for a particle,

$$\frac{d^2 r_i}{dt^2} = \frac{F_i}{m_i} \tag{2}$$

is replaced by

$$\frac{d^2 r_i}{dt^2} = \frac{F_i}{m_i} - \xi\frac{dr_i}{dt} \tag{3}$$

The heat bath parameter ξ can be described as

$$\frac{d\xi}{dt} = \frac{4\pi^2}{\tau_T^2 T_0}(T - T_0) \tag{4}$$

Here, τ_T is the time constant for coupling that determines the relaxation time that the system changes from the instantaneous temperature T to reference temperature T_0. The period for coupling t_{couple} is the time interval between two applications of the temperature coupling method.

dx.doi.org/10.1021/jp5009785 | J. Phys. Chem. A 2014, 118, 8936−8941

RESULTS AND DISCUSSION

Figure 1 shows the autocorrelation functions of thermal noise $C_{noise}(t)$ and their characteristic time τ_{noise} for different computational methods at 300 K. From Figure 1a, we can see that $C_{noise}(t)$ decays exponentially to zero as t increases (from Figure 1b, the exponential function $y(t) = \exp(-t/\tau_{noise})$ can fit $C_{noise}(t)$ quite well). All three $C_{noise}(t)$ with Berendsen, Nose−Hoover, and V-rescale thermostats coincide with each other. When t is ∼10 ps, $C_{noise}(t)$ fluctuates around 0, and simulations show that the autocorrelation time lengths of thermal noise (i.e., the maximum correlation time of thermal noise) are 10 ± 1 ps for these three thermostats at 300 K. The characteristic time τ_{noise} for Berendsen, Nose−Hoover, and V-rescale thermostats are ∼1.92 ps as shown in the inset of Figure 1a. Hence, the influence of different temperature coupling methods on $C_{noise}(t)$ is negligible. Then we changed the value of the coupling parameters for Nose−Hoover thermostat (the results of Berendsen and V-rescale thermostats are presented in Figure S1 of the Supporting Information). In Figure 1b, we changed τ_T from 0.05 to 3 ps (proper integration of the Nose−Hoover thermostat τ_T should be at least 20 times larger than t_{couple}[37]) for Nose−Hoover thermostat and kept t_{couple} = 2 fs. Since $C_{noise}(t)$ values are coinciding with each other for different τ_T, we just draw $C_{noise}(t)$ with τ_T = 0.1 ps in Figure 1b. We can see that the autocorrelation time length of thermal noise is also ∼10 ps. The insert graph of Figure 1b shows that all τ_{noise} fall in the range of 1.92 ± 0.02 ps for different τ_T. In Figure 1c, we changed the other parameter t_{couple} from 2 to 50 fs for Nose−Hoover thermostat and kept τ_T = 1 ps. The $C_{noise}(t)$ values still coincide with each other. The inset of Figure 1c shows that all the τ_{noise} fall in the range of 1.91 ± 0.01 ps. Thus, all these coupling parameters have very limited influence on the autocorrelation behavior of thermal noise. Furthermore, we tested the effect of simulation time step Δt on the behavior of $C_{noise}(t)$. The reference system temperature was kept at 300 K by Nose−Hoover thermostat with τ_T = 0.2 ps and t_{couple} = 6 fs. Figure 1d shows the results of Δt = 0.5, 1, 1.5, and 2 fs. We can see that τ_{noise} is located in the range of 1.90 ± 0.02 ps for different Δt, which indicates that the time step of simulation also has very limited influence on the autocorrelation behavior of thermal noise. All these results show that the autocorrelation behavior of thermal noise is almost unchanged with different temperature coupling methods, parameters, and simulation time steps, and the picoseconds autocorrelation time of thermal noise seems to be intrinsic rather than resulting from the temperature coupling methods. The autocorrelation time length of thermal noise is ∼10 ps with a characteristic time of ∼1.9 ps at 300 K in MD simulation.

Figure 2 shows the influence of the reference temperature T on the autocorrelation behavior of thermal noise with the Nose−Hoover thermostat (τ_T = 0.1 ps and t_{couple} = 2 fs). We can see that $C_{noise}(t)$ changes obviously as T changes. Inset shows that the characteristic time τ_{noise} decreases obviously as the reference temperature T increases, which indicates the dependence of the autocorrelation time length of thermal noise on the reference temperature. Since the reference temperature of the system determines the molecular speed distribution of the Brownian motion, which affects the interaction between neighboring molecules, the autocorrelation time of thermal noise may be correlated with the lifetime of the interaction between neighboring molecules.

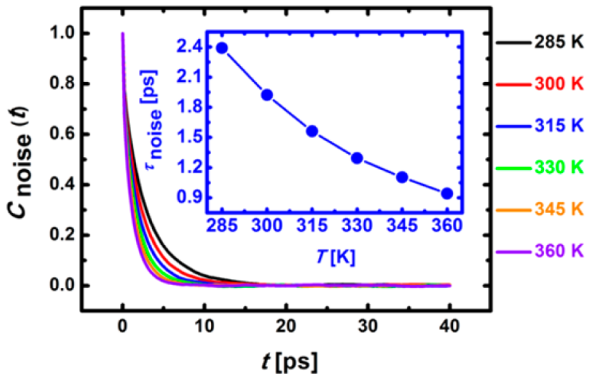

Figure 2. Autocorrelation functions of thermal noises $C_{noise}(t)$ for different reference temperatures T = 285 K (black solid line), 300 K (red solid line), 315 K (blue solid line), 330 K (green solid line), 345 K (orange solid line), and 360 K (violet solid line) by Nose−Hoover thermostat. Inset is the corresponding characteristic time τ_{noise} (blue solid circle).

Hydrogen bonds[46−49] represent the interactions between the neighboring water molecules, which mainly affect the physical properties and chemical properties of water. Thus, we calculated the autocorrelation function of the hydrogen bond,

$$C_{Hbond}(t) = \frac{\langle h(0)\,h(t)\rangle}{\langle h(0)\,h(0)\rangle} \quad (5)$$

where $h(t)$ is the population operator of hydrogen bond, $h(0)$ = 1 represents that the pair of water molecules is bonded at the beginning, and $h(t)$ = 1 means that a pair of water molecules is still bonded at time t, otherwise $h(t)$ = 0. $C_{Hbond}(t)$ was fitted by an exponential function $y(t) = e^{-t/\tau_{Hbond}}$, where τ_{Hbond} was defined as the lifetime of the hydrogen bond.[50−52]

Figure 3 shows the comparison between the autocorrelation behavior of thermal noise and the hydrogen bond. From Figure 3a, we can see that both $C_{noise}(t)$ and $C_{Hbond}(t)$ have the same tendency to decay exponentially, and their autocorrelation time lengths are close to each other. As shown in Figure 3b,c, the parameters of the temperature coupling methods τ_T and t_{couple} have very limited influence on τ_{Hbond} and τ_{noise}. The average values of τ_{Hbond} (1.38 ps) and τ_{noise} (1.92 ps) are quite close. Here we used the definition of the hydrogen bond as oxygen distance of ≤3.5 Å and hydrogen-bond angle of ≤30° in the calculations.[39,40] Since the interaction between hydrogen donor and oxygen acceptor still remains after the breaking of hydrogen bond, the average lifetime of hydrogen bond ought to be smaller than the characteristic time of thermal noise. From Figure 3d, we can see that τ_{Hbond} and τ_{noise} both decrease similarly as T increases. The similar autocorrelation behavior of hydrogen bond and thermal noise suggests that the finite autocorrelation time length of thermal noise is correlated with the finite lifetime of hydrogen bond in water. Since the hydrogen bond represents the interactions between neighboring water molecules, we conclude that the finite autocorrelation time length of thermal noise mainly comes from the finite lifetime of the interactions between neighboring water molecules. The autocorrelation property of thermal noise and hydrogen bond for different water models and simulation packages is still intrinsic. (The results of SPC water model and LAMMPS packages are presented in Figure S2 and Figure S3 of the Supporting Information.)

dx.doi.org/10.1021/jp5009785 | J. Phys. Chem. A 2014, 118, 8936−8941

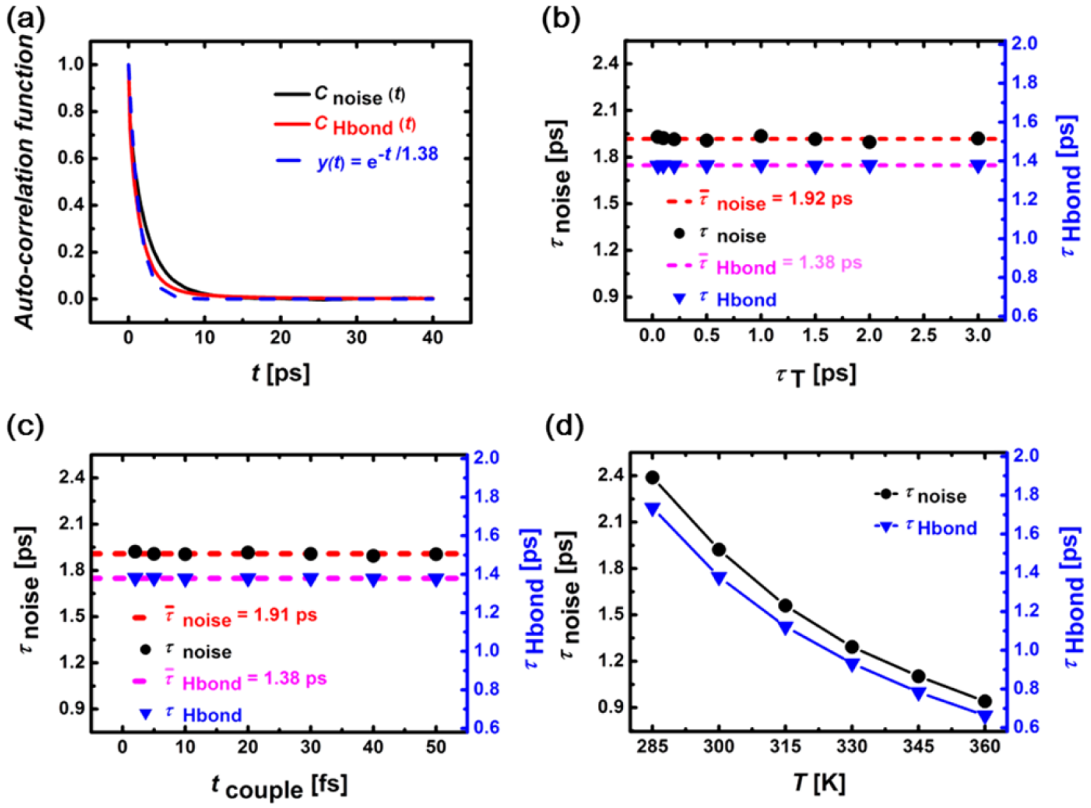

Figure 3. Comparison between the autocorrelation behavior of hydrogen bond and thermal noise. (a) Autocorrelation function of hydrogen bond $C_{Hbond}(t)$ (red solid line) and thermal noise $C_{noise}(t)$ (black solid line) with Nose−Hoover thermostat at 300 K. The blue dash line is the exponential fit $y(t) = \exp(-t/\tau_{Hbond})$ for $C_{Hbond}(t)$, where the $\tau_{Hbond} = 1.38 \pm 0.01$ ps. (b) Characteristic time of thermal noise τ_{noise} (black solid circle) and the lifetime of hydrogen bond τ_{Hbond} (blue inverted triangle) with Nose−Hoover thermostat at 300 K for different τ_T. The red dash line and pink dash line show the average value $\overline{\tau}_{noise} = 1.92$ ps and $\overline{\tau}_{Hbond} = 1.38$ ps. (c) τ_{noise} (black solid circle) and τ_{Hbond} (blue inverted triangle) with Nose−Hoover thermostat at 300 K for different t_{couple}. The red dash line and pink dash line show the average value $\overline{\tau}_{noise} = 1.91$ ps and $\overline{\tau}_{Hbond} = 1.38$ ps. (d) τ_{noise} (black solid circle) and τ_{Hbond} (blue inverted triangle) for different reference temperatures T with Nose−Hoover thermostat.

CONCLUSIONS

We used the MD simulation to investigate the time autocorrelation behavior of thermal noise in water at room temperature. Different temperature coupling methods were used, and we found that the autocorrelation time length of thermal noise is almost independent of the explicit temperature coupling method. This shows that the finite autocorrelation time length at picoseconds for thermal noise in water is intrinsic. Particularly, when the reference temperature is 300 K, thermal noise has an autocorrelation time length of ∼10 ps and a characteristic time of ∼1.9 ps. The autocorrelation time length and the characteristic time of thermal noise depend on the reference temperature: the value of both decreases as the reference temperature increases. Hydrogen bond, which is an important part of interactions between neighboring water molecules, shares a similar autocorrelation behavior with thermal noise; it suggests that the finite autocorrelation time length of thermal noise mainly comes from the finite lifetime of the interactions between neighboring water molecules. The nonwhite behavior of thermal noise may help us to understand the unique transportations at molecular scale.

It should be noted that the explicit value of the autocorrelation time length of thermal noise may be different for different systems; e.g., in the systems containing different solute, the solute may affect the hydrogen bond network of water and have strong interactions with water molecules, which may result in a different autocorrelation time length for thermal noise in these systems. Furthermore, the value of autocorrelation time length of thermal noise may be much larger in the systems with macromolecules, since the macromolecule needs a longer time to regulate the molecular orientation,[53,54] which may enlarge the lifetime of the interactions between neighboring molecules, and the autocorrelation functions may have long nonzero tails. Thus, the unexpected behavior induced by the nonwhite nature of thermal noise may be much easier to be observed in the systems with bigger macromolecules.

ASSOCIATED CONTENT

Supporting Information

Description of Berendsen and V-rescale thermostats, the autocorrelation of thermal noise with different coupling parameters for Berendsen and V-rescale thermostats, and the simulation results for SPC water model and LAMMPS simulation package. This material is available free of charge via the Internet at http://pubs.acs.org.

AUTHOR INFORMATION

Corresponding Author

*E-mail: fanghaiping@sinap.ac.cn. Phone: 021-59554785.

Notes

The authors declare no competing financial interest.

dx.doi.org/10.1021/jp5009785 | J. Phys. Chem. A 2014, 118, 8936−8941

■ ACKNOWLEDGMENTS

We gratefully acknowledge Dr. Chunlei Wang, Dr. Jian Liu, and Dr. Wenpeng Qi for their helpful discussions. This work was supported by the National Natural Science Foundation of China (Grants 11105088, 11175230, and 11290164), the Supercomputer Center for the Chinese Academy of Sciences, and Shanghai Supercomputer Center.

■ REFERENCES

(1) Giulia, C. F.; Gygi, F.; Galli, G. Strongly Anisotropic Dielectric Relaxation of Water at the Nanoscale. *J. Phys. Chem. Lett.* **2013**, *4*, 2477−2481.
(2) Kral, P.; Shapiro, M. Nanotube Electron Drag in Flowing Liquids. *Phys. Rev. Lett.* **2001**, *86*, 131−134.
(3) Ren, J.; Hanggi, P.; Li, B. W. Berry-Phase-Induced Heat Pumping and Its Impact on the Fluctuation Theorem. *Phys. Rev. Lett.* **2010**, *104*, 170601−4.
(4) Leigh, D. A.; Wong, J. K. Y.; Dehez, F.; Zerbetto, F. Unidirectional Rotation in a Mechanically Interlocked Molecular Rotor. *Nature* **2003**, *424*, 174−179.
(5) Kay, E. R.; Leigh, D. A.; Zerbetto, F. Synthetic Molecular Motors and Mechanical Machines. *Angew. Chem., Int. Ed.* **2007**, *46*, 72−191.
(6) Liu, L. Z.; Zhang, J. F.; Zhao, J. J.; Liu, F. Mechanical Properties of Graphene Oxides. *Nanoscale* **2012**, *4*, 5910−5916.
(7) Yang, D.; Huang, W.; He, X. H.; Xie, M. R. Electromagnetic Activation of a Shape Memory Copolymer Matrix Incorporating Ferromagnetic Nanoparticles. *Polym. Int.* **2012**, *61*, 38−42.
(8) Kelly, T. R.; Tellitu, I.; Sestelo, J. P. In Search of Molecular Ratchets. *Angew. Chem., Int. Ed. Engl.* **1997**, *36*, 1866−1868.
(9) Davis, A. P. Tilting at Windmills? The Second Law Survives. *Angew. Chem., Int. Ed.* **1998**, *37*, 909−910.
(10) Kelly, T. R. Progress toward a Rationally Designed Molecular Motor. *Acc. Chem. Res.* **2001**, *34*, 514−522.
(11) Butt, H. J.; Jaschke, M. Calculation of Thermal Noise in Atomic-Force Microscopy. *Nanotechnology* **1995**, *6*, 1−7.
(12) Gong, X. J.; Li, J. Y.; Lu, H. J.; Wan, R. Z.; Li, J. C.; Hu, J.; Fang, H. P. A Charge-Driven Molecular Water Pump. *Nat. Nanotechnol.* **2007**, *2*, 709−712.
(13) Joseph, S.; Aluru, N. R. Pumping of Confined Water in Carbon Nanotubes by Rotation−Translation Coupling. *Phys. Rev. Lett.* **2008**, *101*, 064502-4.
(14) Su, J. Y.; Guo, H. X. Control of Unidirectional Transport of Single-File Water Molecules through Carbon Nanotubes in an Electric Field. *ACS Nano* **2011**, *5*, 351−359.
(15) Bonthuis, D. J.; Horinek, D.; Bocquet, L.; Netz, R. R. Electrohydraulic Power Conversion in Planar Nanochannels. *Phys. Rev. Lett.* **2009**, *103*, 144503-4.
(16) Bonthuis, D. J.; Horinek, D.; Bocquet, L.; Netz, R. R. Electrokinetics at Aqueous Interfaces without Mobile Charges. *Langmuir.* **2010**, *26*, 12614−12625.
(17) Bonthuis, D. J.; Falk, K.; Kaplan, C. N.; Horinek, D.; Berker, A. N.; Bocquet, L.; Netz, R. R. Comment on "Pumping of Confined Water in Carbon Nanotubes by Rotation-Translation Coupling". *Phys. Rev. Lett.* **2010**, *105*, 209401−1.
(18) Suk, M. E.; Aluru, N. R. Comment on "Pumping of Confined Water in Carbon Nanotubes by Rotation-Translation Coupling" Reply. *Phys. Rev. Lett.* **2010**, *105*, 209402−1.
(19) Wong-Ekkabut, J.; Miettinen, M. S.; Dias, C.; Karttunen, M. Static Charges Cannot Drive a Continuous Flow of Water Molecules through a Carbon Nanotube. *Nat. Nanotechnol.* **2010**, *5*, 555−557.
(20) Reimann, P. Brownian Motors: Noisy Transport Far from Equilibrium. *Phys. Rep.* **2002**, *361*, 57−265.
(21) Magnasco, M. O. Forced Thermal Ratchets. *Phys. Rev. Lett.* **1993**, *71*, 1477−1481.
(22) Wan, R. Z.; Hu, J.; Fang, H. P. Asymmetric Transportation Induced by Thermal Noise at the Nanoscale. *Sci. China: Phys., Mech. Astron.* **2012**, *55*, 751−756.
(23) Jiao, Y.; Zhang, F.; Gratzel, M.; Meng, S. Structure−Property Relations in All-Organic Dye-Sensitized Solar Cells. *Adv. Funct. Mater.* **2013**, *23*, 424−429.
(24) Yuan, Q. Z.; Zhao, Y. P. Precursor Film in Dynamic Wetting, Electrowetting, and Electro-Elasto-Capillarity. *Phys. Rev. Lett.* **2010**, *104*, 246101-4.
(25) Comer, J.; Dehez, F.; Cai, W. S.; Chipot, C. Water Conduction through a Peptide Nanotube. *J. Phys. Chem. C* **2013**, *117*, 26797−26803.
(26) Meng, X. W.; Huang, J. P. Enhanced Permeation of Single-File Water Molecules across a Noncylindrical Nanochannel. *Phys. Rev. E* **2013**, *88*, 014104-5.
(27) Xiu, P.; Yang, Z. X.; Zhou, B.; Das, P.; Fang, H. P.; Zhou, R. H. Urea-Induced Drying of Hydrophobic Nanotubes: Comparison of Different Urea Models. *J. Phys. Chem. B* **2011**, *115*, 2988−2994.
(28) Falk, K.; Sedlmeier, F.; Joly, L.; Netz, R. R.; Bocquet, L. Molecular Origin of Fast Water Transport in Carbon Nanotube Membranes: Superlubricity versus Curvature Dependent Friction. *Nano Lett.* **2010**, *10*, 4067−4073.
(29) Phan, A.; Cole, D. R.; Striolo, A. Liquid Ethanol Simulated on Crystalline Alpha Alumina. *J. Phys. Chem. B* **2013**, *117*, 3829−3840.
(30) Deng, Y. H.; Qian, Z. Y.; Luo, Y.; Zhang, Y.; Mu, Y. G.; Wei, G. H. Membrane Binding and Insertion of a pHLIP Peptide Studied by All-Atom Molecular Dynamics Simulations. *Int. J. Mol. Sci.* **2013**, *14*, 14532−14549.
(31) Qiao, Q.; Bowman, G. R.; Huang, X. H. Dynamics of an Intrinsically Disordered Protein Reveal Metastable Conformations That Potentially Seed Aggregation. *J. Am. Chem. Soc.* **2013**, *135*, 16092−16101.
(32) Zhao, H. X.; Kong, X. J.; Li, H.; Jin, Y. C.; Long, L. S.; Zeng, X. C.; Huang, R. B.; Zheng, L. S. Transition from One-Dimensional Water to Ferroelectric Ice within a Supramolecular Architecture. *Proc. Natl. Acad. Sci. U.S.A.* **2011**, *108*, 3481−3486.
(33) Berendsen, H. J. C.; Postma, J. P. M.; Vangunsteren, W. F.; Dinola, A.; Haak, J. R. Molecular-Dynamics with Coupling to an External Bath. *J. Chem. Phys.* **1984**, *81*, 3684−3690.
(34) Nose, S. A Molecular-Dynamics Method for Simulations in the Canonical Ensemble. *Mol. Phys.* **1984**, *52*, 255−268.
(35) Hoover, W. G. Canonical Dynamics—Equilibrium Phase-Space Distributions. *Phys. Rev. A* **1985**, *31*, 1695−1697.
(36) Bussi, G.; Donadio, D.; Parrinello, M. Canonical Sampling through Velocity Rescaling. *J. Chem. Phys.* **2007**, *126*, 014101-7.
(37) Pronk, S.; Pall, S.; Schulz, R.; Larsson, P.; Bjelkmar, P.; Apostolov, R.; Shirts, M. R.; Smith, J. C.; Kasson, P. M.; van der Spoel, D.; Hess, B.; Lindahl, E. GROMACS 4.5: A High-Throughput and Highly Parallel Open Source Molecular Simulation Toolkit. *Bioinformatics* **2013**, *29*, 845−854.
(38) Jorgensen, W. L.; Chandrasekhar, J.; Madura, J. D.; Impey, R. W.; Klein, M. L. Comparison of Simple Potential Functions for Simulating Liquid Water. *J. Chem. Phys.* **1983**, *79*, 926−935.
(39) Hummer, G.; Rasaiah, J. C.; Noworyta, J. P. Water Conduction through the Hydrophobic Channel of a Carbon Nanotube. *Nature.* **2001**, *414*, 188−190.
(40) Wan, R.; Li, J.; Lu, H. J.; Fang, H. P. Controllable Water Channel Gating of Nanometer Dimensions. *J. Am. Chem. Soc.* **2005**, *127*, 7166−7170.
(41) Zhu, F. Q.; Tajkhorshid, E.; Schulten, K. Theory and Simulation of Water Permeation in Aquaporin-1. *Biophys. J.* **2004**, *86*, 50−57.
(42) Kalra, A.; Garde, S.; Hummer, G. Osmotic Water Transport through Carbon Nanotube Membranes. *Proc. Natl. Acad. Sci. U.S.A.* **2003**, *100*, 10175−10180.
(43) Nose, S.; Klein, M. L. Constant Pressure Molecular-Dynamics for Molecular-Systems. *Mol. Phys.* **1983**, *50*, 1055−1076.
(44) Parrinello, M.; Rahman, A. Polymorphic Transitions in Single-Crystals—A New Molecular-Dynamics Method. *J. Appl. Phys.* **1981**, *52*, 7182−7190.
(45) Darden, T.; York, D.; Pedersen, L. Particle Mesh Ewald—An N.Log(N) Method for Ewald Sums in Large Systems. *J. Chem. Phys.* **1993**, *98*, 10089−10092.

(46) Luzar, A.; Chandler, D. Effect of Environment on Hydrogen Bond Dynamics in Liquid Water. *Phys. Rev. Lett.* **1996**, *76*, 928−931.
(47) Arunan, E.; Desiraju, G. R.; Klein, R. A.; Sadlej, J.; Scheiner, S.; Alkorta, I.; Clary, D. C.; Crabtree, R. H.; Dannenberg, J. J.; Hobza, P.; Kjaergaard, H. G.; Legon, A. C.; Mennucci, B.; Nesbitt, D. J. Definition of the Hydrogen Bond. *Pure. Appl. Chem.* **2011**, *83*, 1637−1641.
(48) Markovitch, O.; Agmon, N. The Distribution of Acceptor and Donor Hydrogen-Bonds in Bulk Liquid Water. *Mol. Phys.* **2008**, *106*, 485−495.
(49) Isaacs, E. D.; Shukla, A.; Platzman, P. M.; Hamann, D. R.; Barbiellini, B.; Tulk, C. A. Covalency of the Hydrogen Bond in Ice: A Direct X-ray Measurement. *Phys. Rev. Lett.* **1999**, *82*, 600−603.
(50) Voloshin, V. P.; Naberukhin, Y. I. Hydrogen Bond Lifetime Distributions in Computer-Simulated Water. *J. Struct. Chem.* **2009**, *50*, 78−89.
(51) Luzar, A.; Chandler, D. Hydrogen-Bond Kinetics in Liquid Water. *Nature* **1996**, *379*, 55−57.
(52) Li, J. Y.; Liu, T.; Li, X.; Ye, L.; Chen, H. J.; Fang, H. P.; Wu, Z. H.; Zhou, R. H. Hydration and Dewetting Near Graphite-CH_3 and Graphite-COOH Plates. *J. Phys. Chem. B* **2005**, *109*, 13639−13648.
(53) Sheng, N.; Tu, Y. S.; Guo, P.; Wan, R. Z.; Fang, H. P. Asymmetrical Free Diffusion with Orientation-Dependence of Molecules in Finite Timescales. *Sci. China: Phys., Mech. Astron* **2013**, *56*, 1047−1052.
(54) Tu, Y. S.; Sheng, N.; Wan, R. Z.; Fang, H. P. Inherent Fluctuation-Mediated Equivalent Force Drives Directional Motions of Nanoscale Asymmetric Particles—Surf-Riding of Asymmetric Molecules in Thermal Fluctuations. *arXiv.org, e-Print Arch., Condens. Matter* **2013**, No. 1307.6096.